General Disclaimer

One or more of the Following Statements may affect this Document

- This document has been reproduced from the best copy furnished by the organizational source. It is being released in the interest of making available as much information as possible.

- This document may contain data, which exceeds the sheet parameters. It was furnished in this condition by the organizational source and is the best copy available.

- This document may contain tone-on-tone or color graphs, charts and/or pictures, which have been reproduced in black and white.

- This document is paginated as submitted by the original source.

- Portions of this document are not fully legible due to the historical nature of some of the material. However, it is the best reproduction available from the original submission.

A Sensitive Infrared Imaging Upconverter and Spatial Coherence of Atmospheric Propagation*

R.W. Boyd and C.H. Townes, University of California
Berkeley, California 94720

Theoretical reasoning has indicated that atmospheric "seeing" disturbances should allow sharper astronomical images at infrared than at visible wavelengths,[1] yet imaging devices for astronomy have not generally been available at wavelengths beyond the near infrared. Planets and their atmospheric structure provide interesting subjects for infrared imaging systems,[2] in either broad or narrow spectral regions. So do some more distant objects, such as stars surrounded by thick dust shells, which emit strongly in the infrared, and the nuclei of Seyfert galaxies. All of these objects can be spatially resolved in the larger astronomical telescopes, and hence are valuable subjects for infrared imaging. We describe here the exploration of an infrared imaging technique based on the nonlinear interaction known as upconversion.[3] This technique was used to obtain images of several astronomical objects in the 10 μm spectral region, and to demonstrate quantitatively the sharper images allowed for wavelengths beyond the visible region.

The upconversion process is shown schematically in Figure 1. Infrared radiation is mixed with an intense laser

*This work is supported in part by NASA Grants NGL 05-003-272 and NGR 05-003-452

beam in a nonlinear crystal. The nonlinearity in the optical susceptibility of the crystal generates a signal at the sum frequency, which is in the visible region. The upconversion process in in principle noise free,[4] and thus provides a sensitive method of detecting infrared radiation by first converting it to the visible region where sensitive, low noise detectors are readily available. Figure 1 also illustrates image conversion by upconversion. Photon momentum conservation requires that for each infrared direction of propagation the sum frequency radiation be emitted in a unique direction, and thus a one-to-one correspondence exists between infrared angles of propagation and sum frequency angles of propagation. In fact, the upconversion process simply demagnifies the sum frequency image by approximately the ratio of the sum frequency to the infrared frequency.

In our device, thermal infrared radiation is mixed in a 1 cm long proustite crystal with an 0.25 watt, 0.7525 μm krypton ion laser beam to produce a sum frequency signal at about 0.7 μm (see Figure 2). The 2 cm^{-1} phase matched bandpass of the upconverter can be angle-tuned by tilting the crystal about its y axis to allow operation at any wavelength from 9.0 μ to 11.0 μ. Type II phase matching[5] is used. In order to provide a large usable field of view several hundred spatial modes of the infrared field are simultaneously upconverted. The quantum conversion efficiency obtained with our device was 2×10^{-7}, which was sufficient to allow useful astronomical measurements.

The sum frequency radiation is detected by a Varo 3-stage image intensifier tube, cooled to a temperature of -30 C. Cooling the tube decreases the dark count by a factor of 300 to a level of about 0.1 photo electron per second within the 3 mm field utilized by the upconverter. The output of the image tube is lens-coupled at unit magnification to Kodak TRI-X film for short exposures and to Kodak IIa-D film for long exposures. Some of the laboratory results are shown in Figure 3.

This instrument has been used on the 150 cm McMath solar telescope of Kitt Peak National Observatory. The field of view on the sky is then 40 seconds of arc, and the resolution is limited by diffraction at the telescope aperture and by inhomogeneities in the earth's atmosphere. Resulting images contain several hundred picture elements. Infrared pictures of the Sun, Moon, Mercury, and the dust shell surrounding the star VY CMa have been obtained, and are shown in Figure 4. Integration times range from 4 seconds for the Sun to 15 minutes for VY CMa.

The deleterious effects of atmospheric inhomogeneities on telescope resolution (or "seeing" effects) were studied in the infrared region using this apparatus. The theory of wave propagation in a turbulent medium[1] predicts a $\lambda^{-1/5}$ dependence to the angular resolution of a telescope limited by the effects of seeing when averaged over a sufficiently long time. Previous attempts at verification of this wavelength dependence have met with mixed results, due primarily

to the lack of true imaging devices at long infrared wavelengths where seeing would be expected to be significantly better than in the visible. We have investigated the wavelength dependence of seeing by taking pictures of the sun's limb with the 1.5 m telescope simultaneously at 10 μm and at 0.55 μm, and comparing the sharpness of the solar limb in each case. A typical 10 μm limb profile is shown in Figure 5, and the corresponding visible limb profile is shown in Figure 6. This comparison was repeated a number of times under a variety of atmospheric conditions. After correcting the data for the differences in solar limb darkening[6] and diffraction at the two wavelengths, we found a systematic improvement in seeing at the longer wavelength, as shown in Figure 7. The RMS width of the point spread function for seeing is found to be 1.9 ± .2 times greater at .55 μ than at 10 μ in good agreement with the theoretical value 1.80 predicted on the basis of random turbulence.

These experiments represents the first successful application of imaging upconversion to astronomy. The low (~2 x 10^{-7}) quantum efficiency of the device used severely limited its usefulness as an astronomical detector; nevertheless, these measurements demonstrate the promise of infrared imaging and of upconversion techniques when materials which provide larger nonlinear effects become available.[7]

Figure Captions

Figure 1 Schematic description of the upconversion process (upper). Imaging property of the upconversion process (lower).

Figure 2 Optical layout of the 10 μm imaging upconverter. The monochrometer is used to eliminate background light from the laser discharge tube. Collimated infrared radiation is mixed with the laser beam in the proustite crystal. The interference filters pass the sum frequency while rejecting the laser frequency, providing a factor of 10^{18} discrimination between the two frequencies. The sum frequency image is amplified by the image intensifier tube and recorded photographically.

Figure 3 Upconverted images of several laboratory test objects. Figures a, b, and c show resolution test patterns. The smallest spacing in Figure c is 1.3 times the diffraction limit. Figure d shows a one minute integration on a soldering iron operating at 100 C.

Figure 4 Infrared images of a number of astronomical objects. Computer generated plots of digitized photographic negatives are shown. In each case the field of view is round, and a spurious spot is introduced at the center of the field from the hole in the collimating mirror shown in Figure 2. Note the enhancement in the signal from the subsolar point on

Mercury. The detection of VY Canis Majoris is marginal.

Figure 5 Solar Limb Profile at 10 μm. The solid curve is a theoretical limb profile formed by convolving the true limb profile with a Gaussian shaped point spread function representing the combined effects of "seeing", diffraction, and instrumental resolution. In this case the Gaussian has a full width to 1/e points of 4 arc seconds.

Figure 6 Solar Limb Profile at Visible Wavelengths. The solid curve is a theoretical limb profile formed by convolving the true limb profile with a Gaussian shaped point spread function representing the combined effects of "seeing", diffraction, and instrumental resolution. In this case the Gaussian has a full width to 1/e points of 6 arc seconds.

Figure 7 Visible Seeing vs. Infrared Seeing.

References

1. R.E. Hufnagel and N.R. Stanley, J. Opt. Soc. Am., 54, 52 (1964).

2. J.A. Westphal, K. Matthews, and R.J. Terrile, Ap. J. Lett. 188, L111 (1974).

3. K.F. Hulme, Rep. Prog. Phys., 36, 497 (1973) and F. Zernike and J.E. Midwinter, Applied Nonlinear Optics, John Wiley and Sons, Inc., New York (1973).

4. C.L. Tang, Phys. Rev., 182, 367 (1970).

5. J.E. Midwinter and J. Warner, Br. J. Appl. Phys., 16, 1135 (1965).

6. P. Lena, Astron. Astrophys., 4, 202 (1970) and J.E. Gaustad and J.R. Rogerson, Ap. J., 134, 323 (1961).

7. R.W. Boyd, to be published in Optical Engineering, 1977.

UPCONVERSION PROCESS

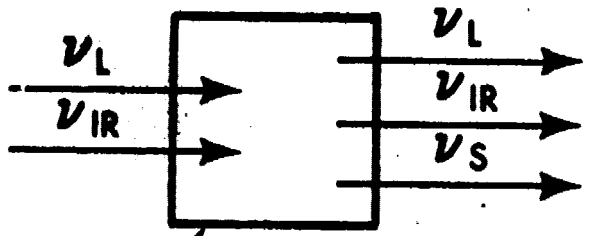

$$\nu_S = \nu_{IR} + \nu_L$$

Proustite crystal

IMAGING PROPERTIES

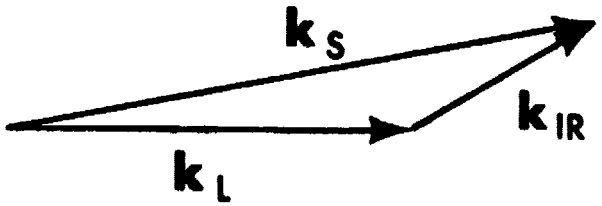

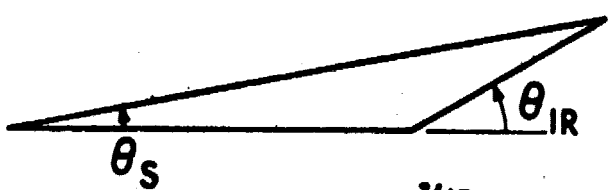

$$\theta_S \sim \theta_{IR} \frac{\nu_{IR}}{\nu_L}$$

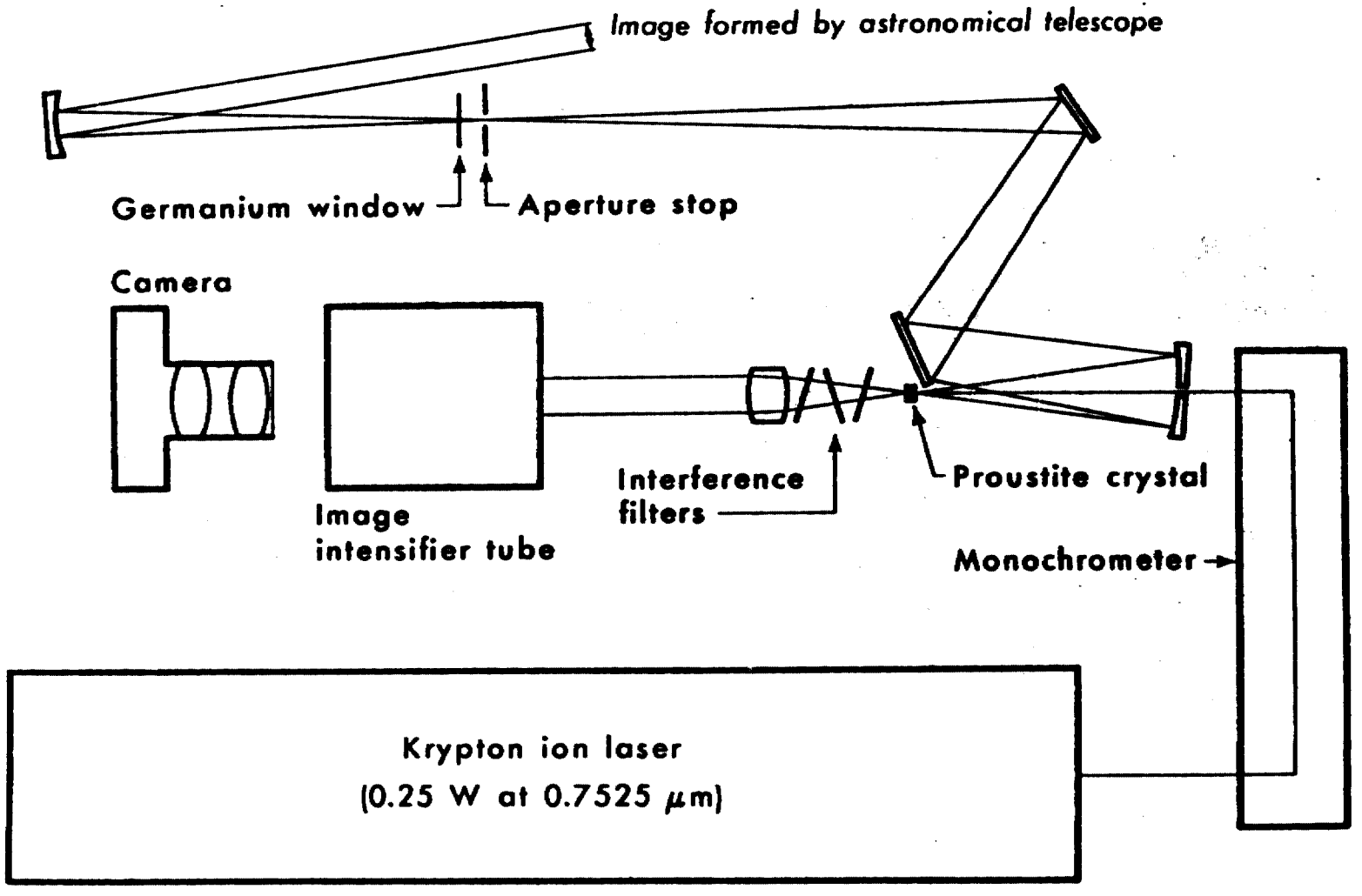
Image formed by astronomical telescope
Germanium window
Aperture stop
Camera
Image intensifier tube
Interference filters
Proustite crystal
Monochrometer
Krypton ion laser
(0.25 W at 0.7525 μm)

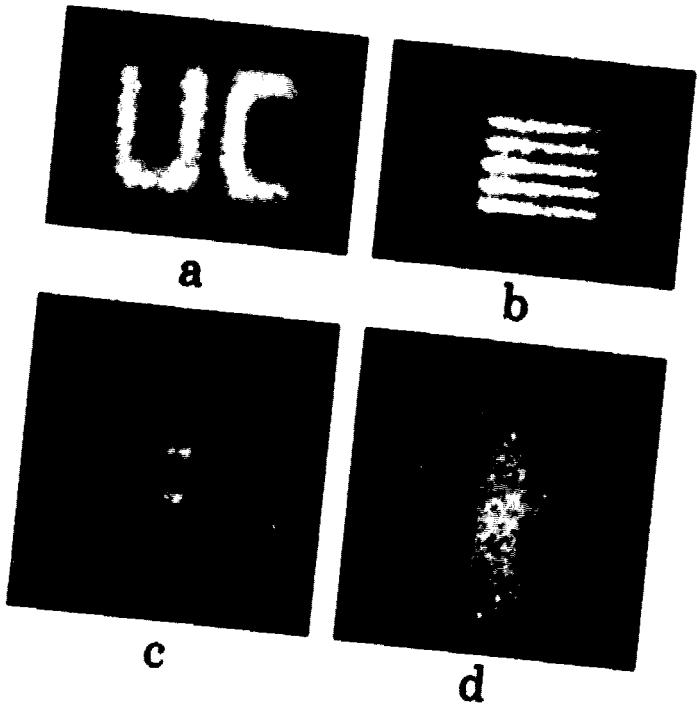

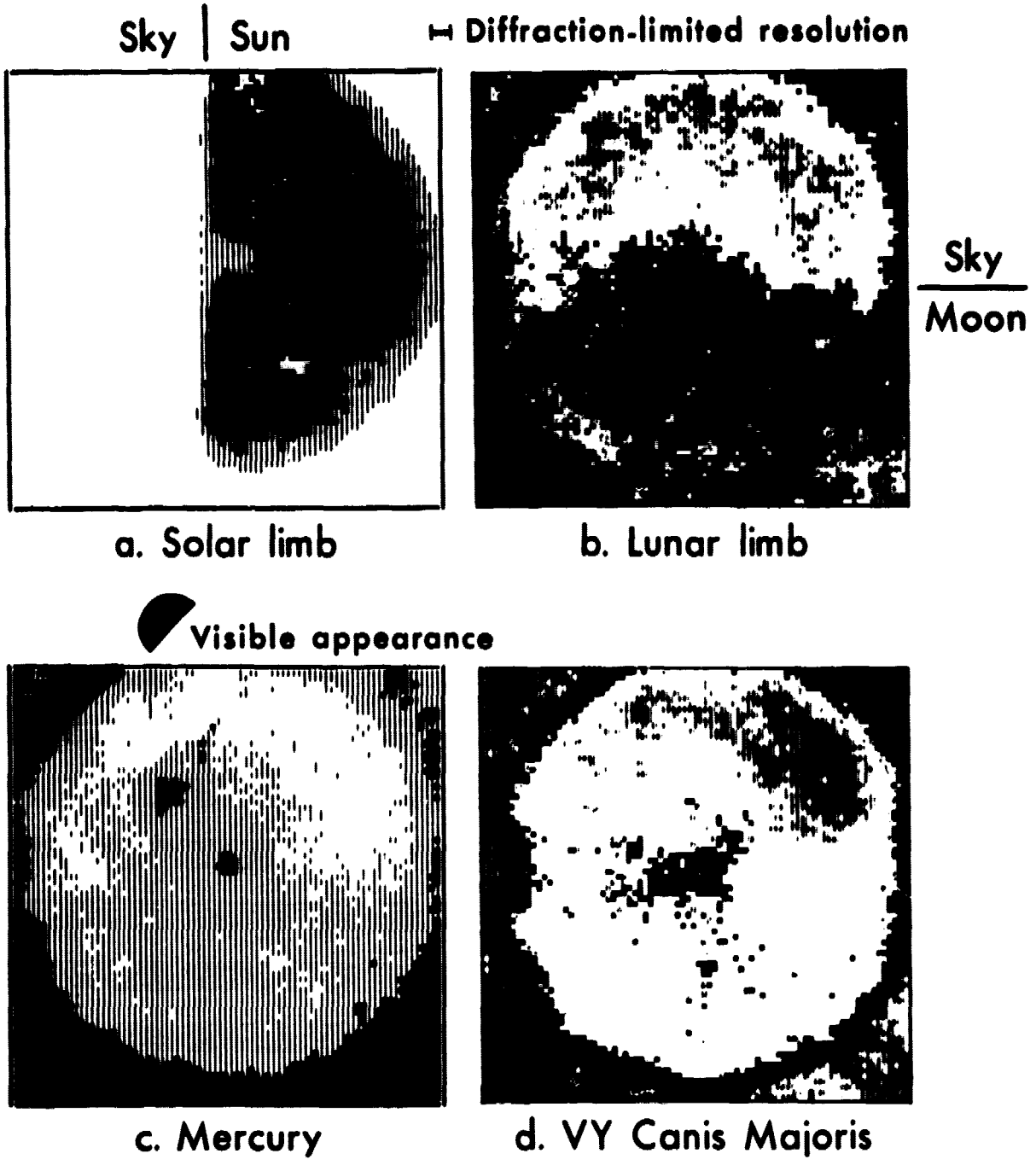
Sky | Sun
Diffraction-limited resolution
Sky
Moon
a. Solar limb
b. Lunar limb
Visible appearance
c. Mercury
d. VY Canis Majoris

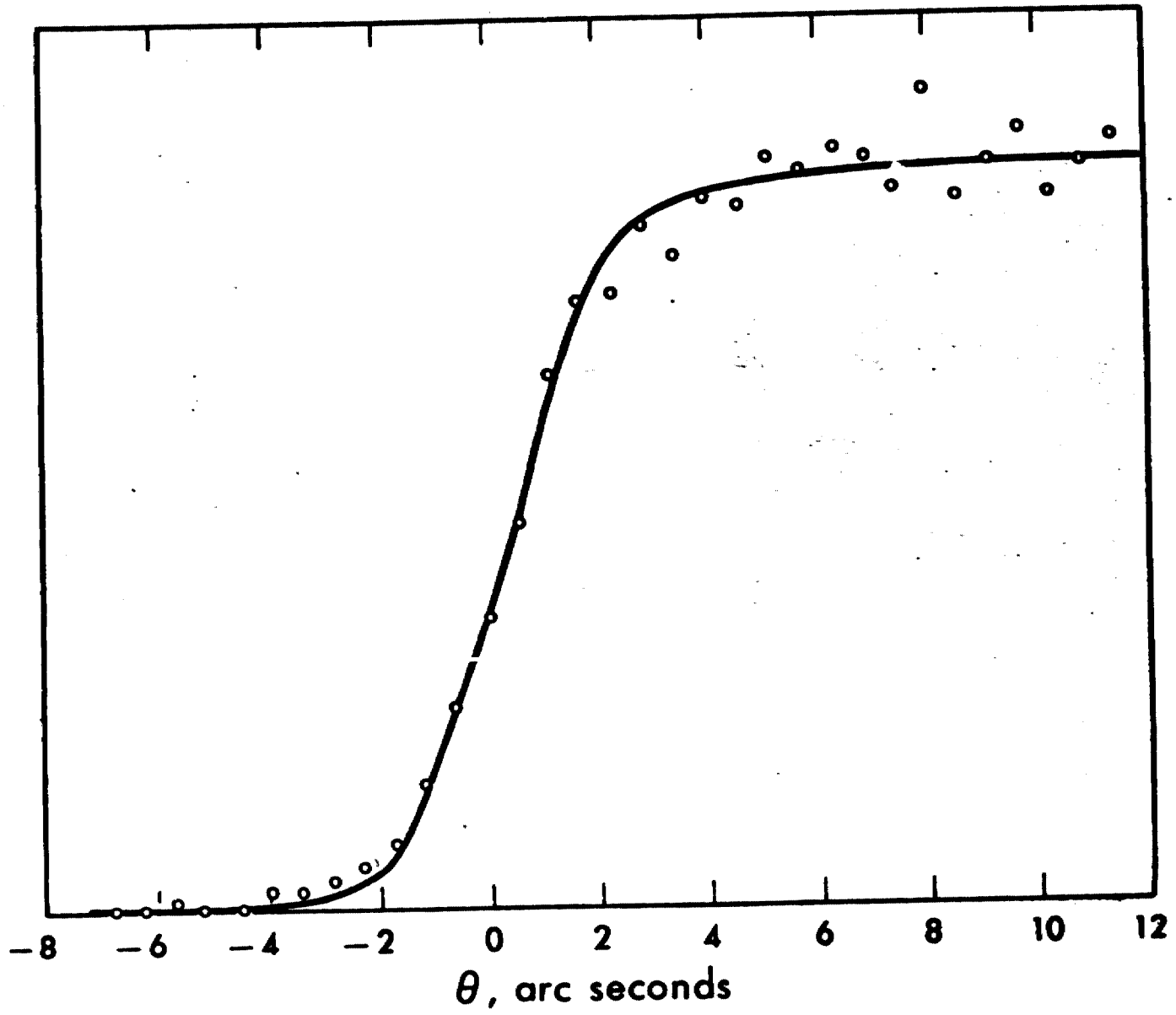
−8
−6
−4
−2
0
2
4
6
8
10
12
θ, arc seconds

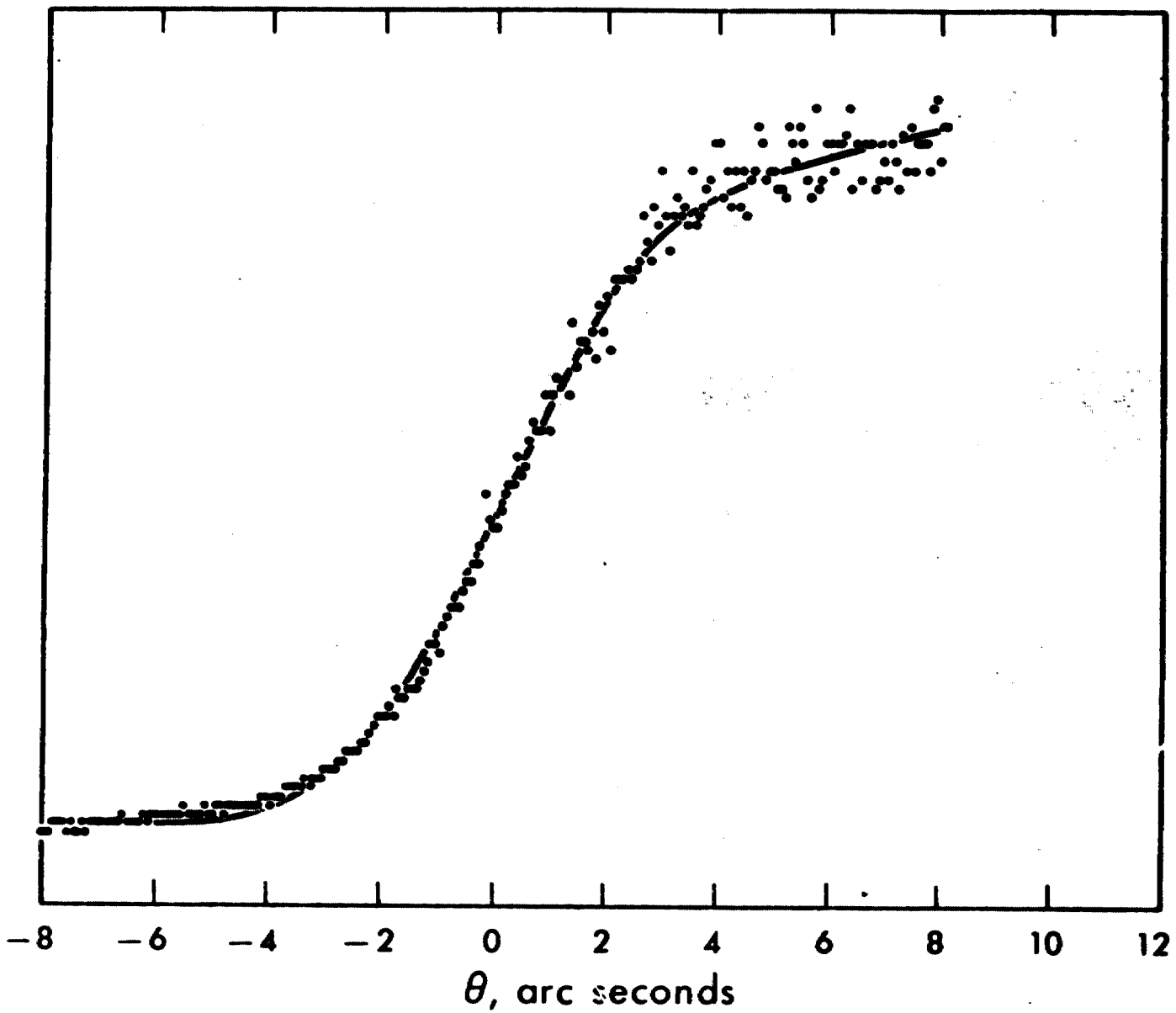
−8
−6
−4
−2
0
2
4
6
8
10
12
θ, arc seconds

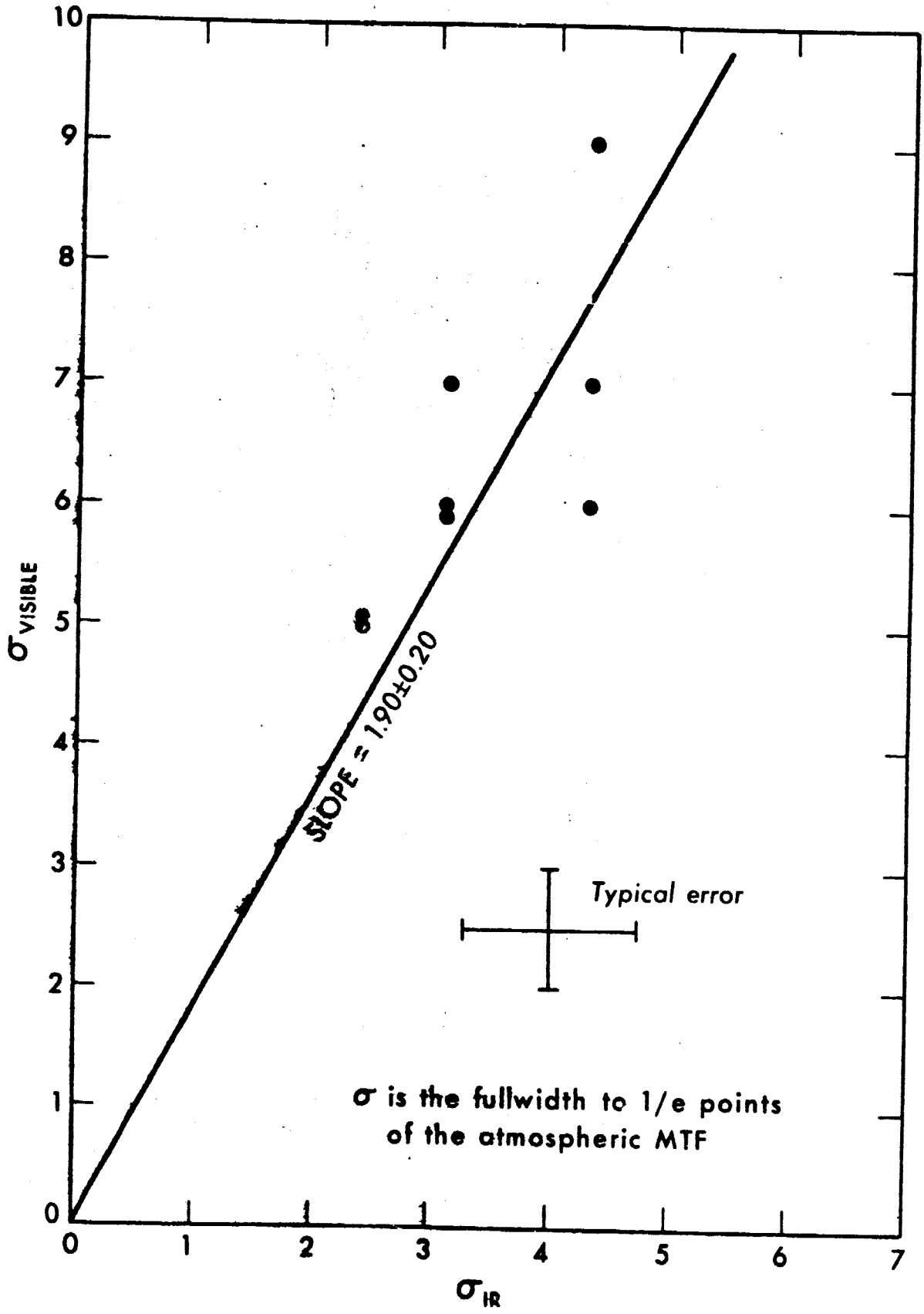
10
9
8
7
6
5
4
3
2
1
0
0
1
2
3
4
5
6
7
σ VISIBLE
σ IR
SLOPE = 1.90±0.20
Typical error
σ is the fullwidth to 1/e points
of the atmospheric MTF